Fabrication of Free-Standing Nanoscale Alumina Membranes with Controllable Pore Aspect Ratios

ARTICLE *in* NANO LETTERS · APRIL 2004

Impact Factor: 13.59 · DOI: 10.1021/nl0348286

4 AUTHORS, INCLUDING:

Chee Seng Toh
Nanyang Technological University
53 PUBLICATIONS **961** CITATIONS

SEE PROFILE

NANO LETTERS

2004
Vol. 4, No. 5
767−770

Fabrication of Free-Standing Nanoscale Alumina Membranes with Controllable Pore Aspect Ratios

Chee-Seng Toh, Brendan M. Kayes, E. Joseph Nemanick, and Nathan S. Lewis*

Division of Chemistry and Chemical Engineering 127-72, California Institute of Technology, Pasadena, California 91125

Received September 25, 2003; Revised Manuscript Received March 22, 2004

ABSTRACT

Porous alumina films with controllable pore sizes and having submicrometer film thicknesses were fabricated by the anodization of Al overlayers. The Al was deposited by sputtering onto either glass or onto silicon that had been coated with a layer of silicon nitride. Alumina membranes having thicknesses between 300 and 1000 nm were prepared analogously using a lithographic process to produce free-standing porous alumina films that were peripherally supported on a 500-μm-thick silicon substrate.

Alumina structured with nanometer-sized pores has attracted significant recent attention as a template for the fabrication of nanostructures.[1−3] The formation of nanoporous alumina is generally performed by anodizing Al under a bias of 10−100 V in acidic media such as sulfuric acid, phosphoric acid, or oxalic acid.[4−8] This process produces a thin alumina barrier layer overlaid by a highly ordered hexagonal prismatic structure having a pore at the center of each hexagon. Variation in the electrochemical and etching conditions can provide control over the pore density and pore diameter, with available pore sizes between 10 and 200 nm.[7,9] Precise control of the channel growth process has been achieved using mechanical imprinting techniques to create nanosized indentations on the aluminum metal surface[10] or alternatively through the use of electron-beam[11] or focused-ion-beam lithographic methods.[12] The high structural regularity of the films produced by the electrochemical formation of porous alumina has been exploited as a template for the fabrication of nanowires of metals,[13,14] carbons,[15,16] polymers,[17] and semiconductors.[18,19] Porous alumina derived from thermally evaporated or sputtered aluminum films has also recently been used as a lithographic mask for the fabrication of microstructures on metals and semiconductors.[1,2] However, many potential applications of porous alumina require nanometer-scale film thicknesses that additionally provide access to a completely porous support structure with no remaining alumina barrier layer. Furneaux et al. described the use of progressive reduction in the anodizing voltage to create a perforation of the barrier layer and to achive separation of the alumina film from the aluminum, resulting in a porous micrometer-thick free-standing membrane.[20] Masuda et al. used the porous alumina as a template for making free-standing micrometer-thick metal films through a two-step replication process.[21] We describe herein an approach to making such free-standing nanoporous alumina membranes with controllable pore sizes and thicknesses in the nanometer regime, with the membranes peripherally supported on 500-μm-thick Si substrates to provide mechanical strength to the overall device design.

Aluminum films were produced by magnetron sputtering (80 W; power density of 7.1 W cm^{-2}) using a 99.999% Al target in an atmosphere of research-grade Ar at 5×10^{-3} Torr. Substrates were either glass microscope slides (Corning) or (100) oriented, 13−23 Ω-cm resistivity, 500−550-μm-thick silicon wafers (Silicon Quest) that had been coated with 30 ± 2 nm of silicon nitride. The samples were placed on a rotating stage to ensure a uniform coverage of the Al layer. Sputtering conditions were optimized to produce uniform Al films with 200−500 nm grain sizes. All of the portions of the aluminum-coated silicon substrates that contained exposed Si, including the edges of the devices, were then coated with either epoxy glue or varnish to minimize electrochemical reactions of the Si itself. For substrates having a (delicate) 30-nm-thick silicon nitride membrane, varnish was applied generously to the back (silicon nitride) side of the window and was allowed to dry for 60 min in air prior to the anodization procedure. An alligator clip was used to connect the Al on the front side of the substrate to a dc power supply; the anodization voltage was applied between the Al and a Pt gauze counterelectrode. Anodization was performed at room temperature (∼20 °C) for 7 min at 40 V in 0.10 M oxalic acid (aq). The anodized film was then rinsed with 18 MΩ-cm resistivity water and immersed for 5 min in an aqueous solution that contained

* To whom correspondence should be addressed. E-mail: nslewis@caltech.edu. Fax: 626-395-8867.

10.1021/nl0348286 CCC: $27.50
Published on Web 04/23/2004

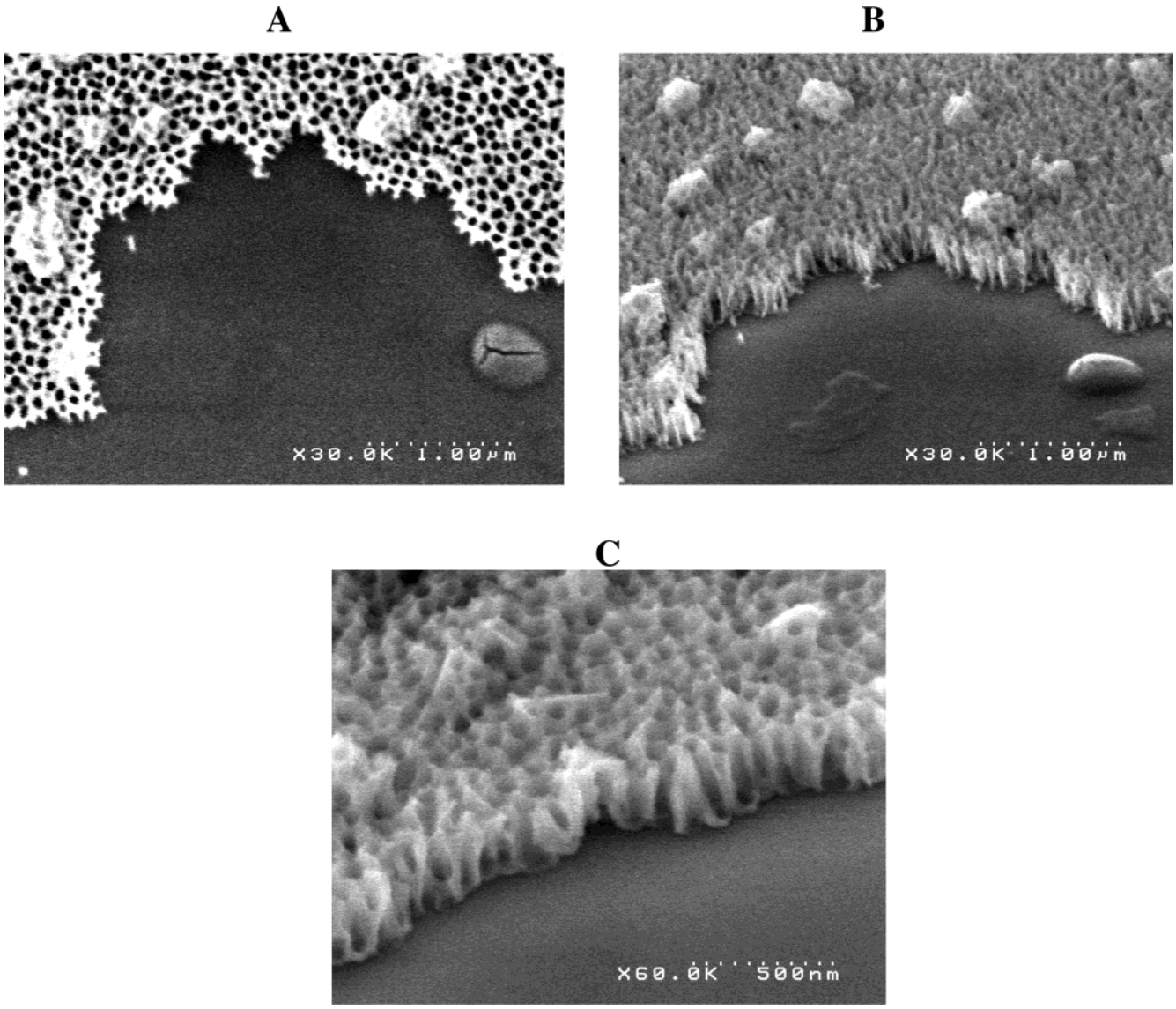

Figure 1. Field-emission scanning electron micrograph images of (A) surface morphology and (B, C) side profiles of a 300-nm-thick nanoporous alumina film supported on a silicon nitride-coated silicon substrate. The same morphologies were observed for alumina prepared from aluminum sputtered onto glass substrates.

0.20 M chromic acid and 0.30 M H_3PO_4. The film was then rinsed with H_2O, dried in air, and reanodized at 40 V for 7 min in the oxalic acid solution. After the second anodization step, the device was rinsed with H_2O, and the varnish was removed by immersion in acetone. Pore widening was carried out at room temperature by controlled time exposure to a solution of 0.4 M phosphoric acid (aq).

Figure 1A shows a field-emission scanning electron micrograph (FE-SEM) of the surface morphology of a 300-nm-thick nanoporous alumina film. This film was prepared by the anodization of an aluminum film that had been sputtered onto a silicon nitride-coated Si substrate, but the same morphology was observed from the anodization of Al films sputtered onto glass substrates. The pores were relatively uniform in size, and a sampling of 100 pores in the film of Figure 1A yielded values for the distribution of maximum and minimum elliptical pore diameters of 68.1 ± 10.1 and 50.4 ± 7.0 nm, respectively. The same degree of regularity was obtained in alumina films as thick as 1.0 μm (not shown). Using a combination of physical sputtering and chemical etching techniques, the aspect ratios of pores within the anodized alumina films could be controlled. The pore lengths within the resulting anodized alumina films were varied by changing the sputtering time used to deposit the aluminum. The diameters of the pores were increased up to ~200 nm by etching the alumina films in phosphoric acid solutions having a concentration between 0.30 and 0.50 M.

At an anodization voltage of 100 V, pores could not be formed by the anodization of sputtered aluminum films that were less than 250 nm thick. Similarly, at an anodization voltage of 40 V, pores could not be formed using sputtered Al films that were thinner than 200 nm. This limitation occurred because the formation of alumina by the anodization of Al produces a porous Al_2O_3 layer on top of a nonporous barrier Al_2O_3 layer, with alumina films that were prepared by the anodization of Al sheets yielding a barrier-layer growth parameter of 1.0−1.4 nm V^{-1}.[4,22] Figure 1C shows that the sample prepared with an anodization voltage of 40

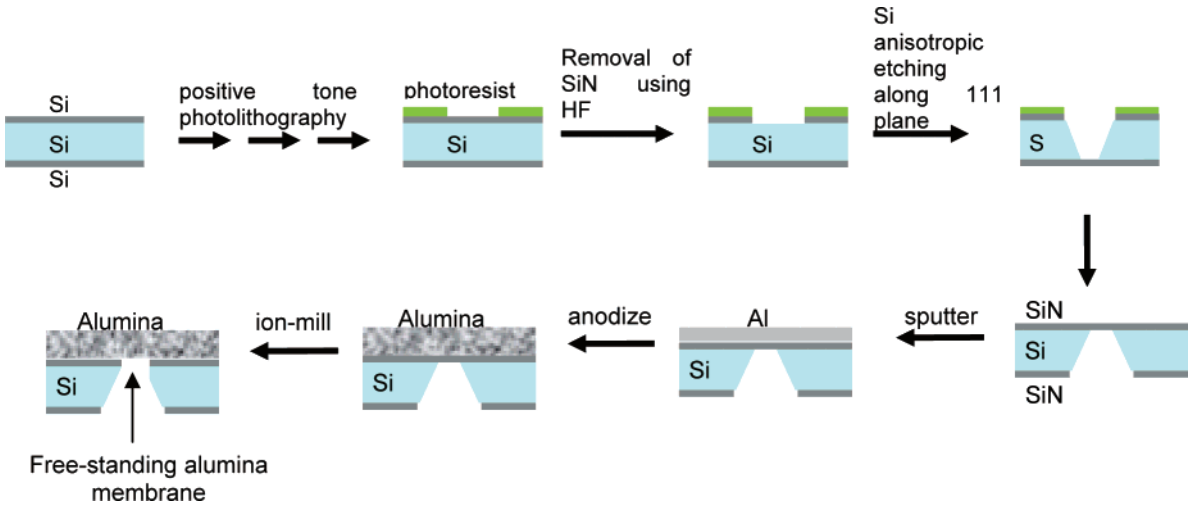

Figure 2. Process for making free-standing alumina membranes supported on Si substrates.

V[4,22] had a barrier layer thickness between 25 and 75 nm. The experimentally observed thickness limit of the Al film for the successful formation of porous alumina was about 100 nm larger than the barrier-layer thickness, which is consistent with expectations for the loss of aluminum ions into the bulk solution during anodization under acidic conditions. Submicrometer-thick porous alumina films can thus be prepared provided that the initial Al film thickness is greater than the thickness of the barrier layer.

Submicrometer-thick free-standing alumina membranes supported on 500-μm-thick silicon substrates were fabricated by implementing the additional process steps outlined schematically in Figure 2. First, positive-tone photolithography was used to produce 40 holes (each 0.5 $\times$ 0.5 mm^2) in a layer of photoresist that had been deposited onto a Si substrate. The exposed silicon nitride was then removed using 2.4 M HF(aq). In the next step, the underlying silicon was exposed to 16 M KOH(aq), which etched the silicon at 54.7° angles relative to the surface normal (i.e., along the (111) planes). The etch stop provided by the underlying silicon nitride layer produced a silicon nitride membrane device with a window whose dimensions were determined by those of the initial photolithographic mask along with the known angle of the etch and the thickness of the Si wafer. Typically, 10−15 intact silicon nitride membrane devices were obtained from the processing of 40 regions in a single Si wafer. An Al layer of the desired thickness was then sputtered onto the remaining silicon nitride membranes on these devices.

Two approaches were explored to prepare submicrometer-thick alumina membranes from this Al film. Ion milling of the silicon nitride below the aluminum, followed by anodization to create pores, was not successful because the ultrathin alumina membrane was unstable during the anodization process. This instability of the ultrathin aluminum and/or alumina membrane is presumably due to a localized increase in temperature that occurs during anodization and/or to effects of stress across the film, as observed by Chu et al. for micrometer-thick alumina films formed on glass substrates that had been coated with tin-doped indium oxide.[23] In contrast, the anodization of the aluminum followed by the removal of the silicon nitride by ion milling was successful (Figure 2). The presence of an underlying silicon nitride membrane helped keep the aluminum film and resulting alumina membrane intact during and after the anodization process. An additional varnish coating on the silicon nitride prior to anodization reduced the breakage rate of the aluminum and of the alumina membrane from an initial 90% (9 out of 10 samples) to ~10% (1 out of 12 samples).

Once the aluminum had been anodized, ion milling was used to remove, in the exposed window region, both the silicon nitride membrane support and the barrier layer in the anodized alumina layer. For this purpose, the argon ion beam was directed at normal incidence onto the back (silicon nitride) side of the devices. Argon-ion milling was performed at an Ar pressure of 1 $\times$ 10^{-4} Torr in a chamber having a base pressure of 8 $\times$ 10^{-9} Torr. An Iontech 3-cm ion source was employed with a beam current of 20 mA and a beam voltage of 500 V. The etching rate was controlled via the ion current density, the distance between the substrate and the ion gun, and the grazing angle of the ion beam relative to the substrate. The ion-milling process was first optimized and calibrated using silicon nitride-coated silicon substrates, followed by a test run on one alumina device where the progress of silicon nitride and alumina barrier-layer removal by ion milling was monitored using FE-SEM. Finally, ion milling was carried out on 10 alumina devices for an initial 15 s, followed by milling for additional 60-s time periods as warranted, and the progress was monitored at each stage by FE-SEM. Figure 3 shows the change in surface morphology of the silicon nitride membrane as viewed from the back (window) side of the device as a function of the ion-milling time. After ~7 min of ion milling, the silicon nitride and the alumina barrier had both been removed, and the nanoporous structure of the underlying alumina below the silicon nitride layer was clearly evident. FE-SEM measurements for one alumina device indicated that the pore densities of the back and front sides of the resulting alumina membrane were 125.3 $\pm$ 10.3 and 123.7 $\pm$ 20.9 pores μm^{-2}, respectively, with pore diameters between 49.5 $\pm$ 2.7 and 34.6 $\pm$ 1.8 nm.

In conclusion, the approach described above allows the formation of nanoporous alumina membranes of submicrometer thickness, with the ability to control the aspect ratios

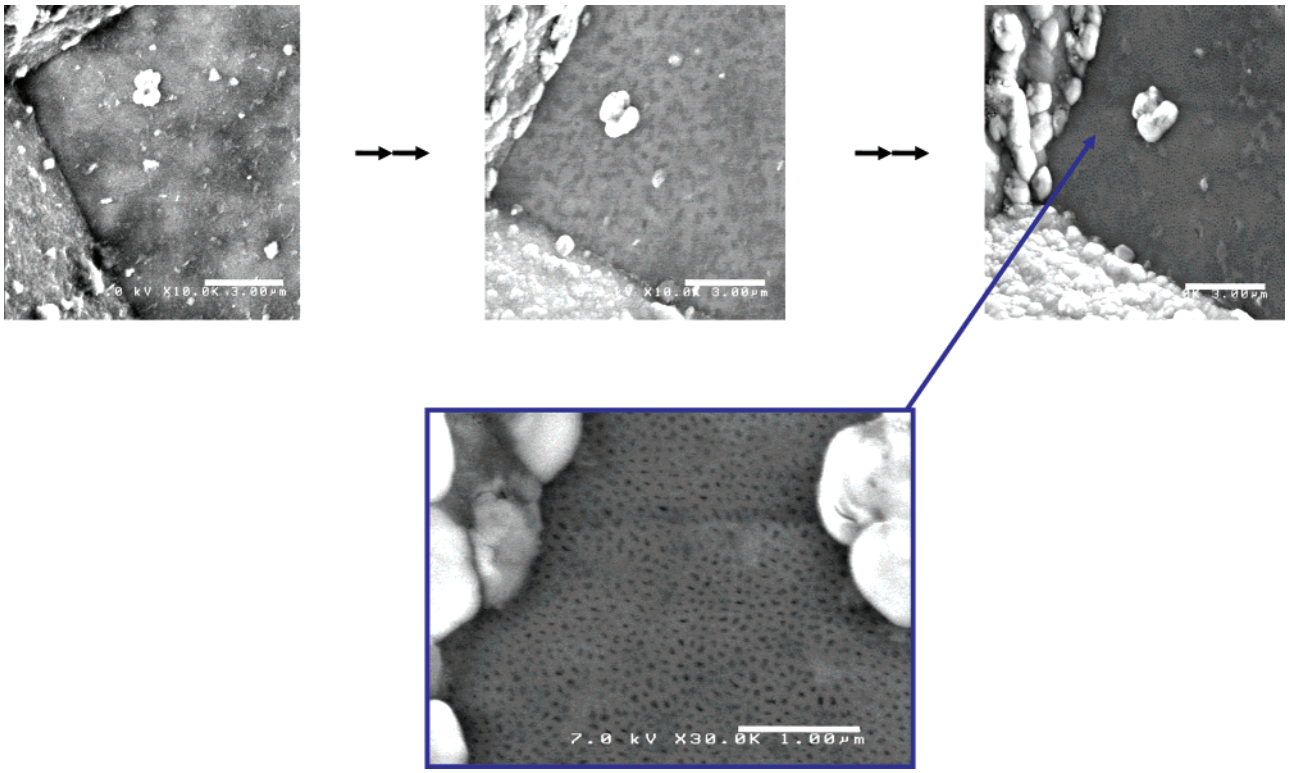

Figure 3. Scanning electron micrographs of the back (window) side of one silicon device after various ion-milling time periods, revealing the nanosized pores after ~7 min of ion milling.

of the resulting pores and with no barrier layer, which if present would preclude the transport of ions or other chemical species through the entire device. These submicrometer-thick membrane devices ought to extend the types of applications that currently use commercial 60-μm-thick alumina membranes, including filtration, controlled diffusion of analytes, and cell culture supports, and should enable applications currently not achievable with alumina membranes >10 μm in thickness. These include the construction of photovoltaic junctions, photoelectrochemical microassemblies, or separators for microfuel cells, in which ionic and/or electronic motion over macroscopic distances is a significant loss mechanism. These submicrometer-thick membrane devices should also serve as good templates for the growth of nanostructures of polymers, metals, and semiconductors that have to date been implemented in 60-μm-thick alumina membranes or in >10-μm-thick anodically grown alumina membranes prepared from the anodization of either aluminum sheets[13,15,17−19] or sputtered aluminum films.[23,24]

Acknowledgment. We acknowledge the National Science Foundation (grant CHE-0213589) for supporting this work and the National University of Singapore for providing a fellowship to C.S.T. We also thank J. Casperson for assistance with the ion-milling process.

References

(1) Crouse, D.; Lo, Y. H.; Miller, A. E.; Crouse, M. *Appl. Phys. Lett.* **2000**, *76*, 49−51.
(2) Mozalev, A.; Surganov, A.; Magaino, S. *Electrochim. Acta* **1999**, *44*, 3891−3898.
(3) Almawlawi, D.; Bosnick, K. A.; Osika, A.; Moskovits, M. *Adv. Mater.* **2000**, *12*, 1252−1257.
(4) Keller, F.; Hunter, M. S.; Robinson, D. L. *J. Electrochem. Soc.* **1953**, *100*, 411−419.
(5) Hunter, M. S.; Fowle, P. *J. Electrochem. Soc.* **1954**, *101*, 481−485.
(6) Gerischer, H. *Angew. Chem., Int. Ed. Engl.* **1958**, *70*, 285−297.
(7) Diggle, J. W.; Downie, T. C.; Goulding, C. W. *Chem. Rev.* **1969**, *69*, 365−405.
(8) Goad, D. G. W.; Moskovits, M. *J. Appl. Phys.* **1978**, *49*, 2929−2934.
(9) O'Sullivan, J. P.; Wood, G. C. *Proc. R. Soc. London, Ser. A* **1970**, *317*, 511−543.
(10) Masuda, H.; Yamada, H.; Satoh, M.; Asoh, H.; Nakao, M.; Tamamura, T. *Appl. Phys. Lett.* **1997**, *71*, 2770−2772.
(11) Li, A. P.; Muller, F.; Gosele, U. *Electrochem. Solid State Lett.* **2000**, *3*, 131−134.
(12) Liu, C. Y.; Datta, A.; Wang, Y. L. *Appl. Phys. Lett.* **2001**, *78*, 120−122.
(13) Cepak, V. M.; Hulteen, J. C.; Che, G. L.; Jirage, K. B.; Lakshmi, B. B.; Fisher, E. R.; Martin, C. R. *J. Mater. Res.* **1998**, *13*, 3070−3080.
(14) Shingubara, S.; Okino, O.; Sayama, Y.; Sakaue, H.; Takahagi, T. *Solid-State Electron.* **1999**, *43*, 1143−1146.
(15) Che, G. L.; Lakshmi, B. B.; Fisher, E. R.; Martin, C. R. *Nature* **1998**, *393*, 346−349.
(16) Kyotani, T.; Pradhan, B. K.; Tomita, A. *Bull. Chem. Soc. Jpn.* **1999**, *72*, 1957−1970.
(17) Parthasarathy, R. V.; Martin, C. R. *Nature* **1994**, *369*, 298−301.
(18) Lakshmi, B. B.; Patrissi, C. J.; Martin, C. R. *Chem. Mater.* **1997**, *9*, 2544−2550.
(19) Hoyer, P. *Langmuir* **1996**, *12*, 1411−1413.
(20) Furneaux, R. C.; Rigby, W. R.; Davidson, A. P. *Nature* **1989**, *337*, 147−149.
(21) Masuda, H.; Nishio, K.; Baba, N. *Thin Solid Films* **1993**, *223*, 1−3.
(22) Wood, G. C.; Osulliva. Jp; Vaszko, B. *J. Electrochem. Soc.* **1968**, *115*, 618−626.
(23) Chu, S. Z.; Wada, K.; Inoue, S.; Todoroki, S. *J. Electrochem. Soc.* **2002**, *149*, B321−B327.
(24) Chu, S. Z.; Wada, K.; Inoue, S.; Todoroki, S. *Chem. Mater.* **2002**, *14*, 266−272.

NL0348286